Supporting Information

Zhang et al. 10.1073/pnas.1323977111

SI Materials and Methods

Chemicals and Reagents. Both cholic acid (CA) and chenodeoxycholic acid (CDCA) were purchased from Sigma. Rabbit anti-aquaporin 2 (AQP2) was from Millipore (AB3066). Mouse anti-farnesoid X receptor (FXR) was from Perseus Proteomics. Rabbit anti-histone antibody was from Cell Signal Technology. Primary antibodies against AQP1, Tamm–Horsfall glycoprotein (THP), sodium-chloride cotransporter (NCC) used in the present study were purchased from Santa Cruz Biotechnology. Adenoviruses expressing FXRα1 (Ad-FXRα1), FXRα2 (Ad-FXRα2) and their control adenoviruses (Ad-VP16) were kindly provided by Peter Edwards at University of California, Los Angeles.

mRNA Isolation, RT-PCR, and Real-Time PCR. Total mRNA was isolated with a commercial mRNA isolation kit (Biotek). mRNA samples were reverse-transcribed to cDNA with RevertAidTM First Strand cDNA Synthess Kit (Fermentas). cDNA was used as template in the PCR reaction with SYBR Green 1 (Bio-rad). The following primers were used: *AQP2*_forward: 5′-TTG CCA TGT CTC CTT CCT TC-3′; *AQP2*_reverse: 5′-GGT CAG GAA GAG CTC CAC AG-3′; *FXRα*_forward: 5′- CCG AGA GAA GAA CCG AGT T-3′; *FXRα*_reverse: 5′- TAG ATG CCA GGA GAA TAC CAG-3′; *FXRβ*_forward: 5′-ATG CAG TTT CAG GGC TTA GAA-3′; *FXRβ*_reverse: 5′-CGG GAC ATT GTT GTA TGG G-3′; *β-actin*_forward: 5′-TGT TAC CAA CTG GGA CGA CA-3′; *β-actin*_reverse: 5′-GGG GTG TTG AAG GTC TCA AA-3′; *18S*_forward: 5′-GAA ACG GCT ACC ACA TCC AAG G-3′; *18S*_reverse: 5′-GCC CTC CAA TGG ATC CTC GTT A-3′. The PCR reaction were carried out at 94 °C for 5 min, followed by 35 cycles of 94 °C for 30 s, 59 °C for 30 s, 72 °C for 30 s, with a final extension at 72 °C for 5 min. *β-Acti*n and *18S* were used as an internal control.

Protein Extraction and Western Blot Analysis. Kidney or cell proteins were solubilized in the lysis buffer (20 mM Tris-Cl, pH 7.4, 1 mM EDTA, 0.1% SDS, 1% Triton X-100) containing phosphatase inhibitor (P1260, PPLYGEN) and 0.2 mg/mL PMSF. Nuclear extracts were isolated using the NE-PER Kit according to the manufacturer's instructions (78833, Pierce Biotechnology, Inc.). Protein concentrations were determined by the bicinchoninic acid assay (P001, Vigorous Biotechnology). 40∼80 μg proteins mixed with loading buffer were separated on a 10% (wt/vol) SDS/PAGE gel and transferred to a nitrocellulose membrane. The membrane was blocked with 5% (wt/vol) skim milk and subsequently incubated with selected primary antibodies overnight at 4 °C. The primary antibodies used in this study were mouse anti-FXR (1:1000); rabbit anti-AQP2 (1:1000); mouse anti–β-actin (1:1000). After washes, the membrane was incubated for 1 h at room temperature with HRP-conjugated secondary antibodies (Santa Cruz Biotechnology). After washing the membrane again, antibody binding was detected using chemiluminescence substrate (sc-2048, Santa Cruz Biotechnology) followed by exposure to X-ray film (Kodak XBT-1).

Immunofluorescence. Kidneys were embedded and cryosections were mounted on polylysine-coated slides and fixed with ice-cold acetone for 10 min. After rinsing three times with PBS, sections were permeabilized in 0.1% Triton X-100 in PBS for 10 min and blocked by 0.5% BSA in PBS for 10 min. The sections were then incubated with primary antibodies overnight at 4 °C. After washes, the sections were incubated with appropriate DyLight 488 (green) or DyLight 594 (red)-conjugated secondary antibodies (Jackson ImmunoResearch Laboratories) for 1 h at room temperature. Nuclei were stained with DAPI. Images were obtained through a confocal microscope. Culture primary inner medullary collecting duct (IMCD) cells were fixed with 4% (wt/vol) paraformaldehyde (PFA) for 15 min at room temperature on a rocking platform and then were subjected to immunofluorescence staining.

Immunohistochemistry. For immunohistochemistry studies, kidneys were fixed with 4% (wt/vol) PFA in PBS, dehydrated, and embedded in paraffin. Then the kidneys were sectioned (4 μm) and incubated with selected primary antibodies overnight at 4 °C. Then, the sections were incubated with horseradish-peroxidase-conjugated secondary antibody (Zhong-shan Golden Bridge) for 30 min at 37 °C. The slides were counterstained with hematoxylin.

Microarray Analysis. Mouse kidney gene expression profile of each sample was examined by the use of the mouse genome oligonucleotide microarray (Affymetrix Gene Chip Mouse Genome 430 2.0 Array, Affymetrix). Significant fold change among genes was determined by taking the ratio of the expression between CDCA treated group versus control group. A differentially expressed gene was defined as a variation in gene expression more than 1.5-fold and a detection P value < 0.05 (t test).

dDAVP Treatment. Male $FXR^{+/+}$ and $FXR^{-/-}$ mice were injected i.p. with 1 μg/kg of dDAVP (Sigma) in saline. The bladders were emptied by massage to collect urine. At the same time, water bottle was removed from the cage. Then spot urine was collected by bladder massage at the indicated times.

Measurement of Fasting Blood Glucose Levels. Mice were fasted overnight. Then blood glucose levels were determined by the use of a Freestyle Brand Glucometer (Roche) with blood collected from the tail vein.

Primary Culture of Mouse IMCD Cells. Primary mouse IMCD cells were cultured as described previously with minor modifications (1). Briefly, kidney medullas of male mice (4∼6 wk) were dissected and transferred to hyperosmotic medium (Dulbecco's Modified Eagle Medium-Ham's F12 medium with 120 mM NaCl and 80 mM urea added). After mincing, the medullas were digested in the enzyme solution (12 mL hyperosmotic medium plus 24 mg collagenase B and 8.5 mg hyaluronidase) for 60∼90 min at 37 °C under continuous agitation. The cell suspension was then centrifuged and the pellet was washed three times by prewarmed, enzyme-free hyperosmotic medium before seeding. The cells were treated with hyperosmotic medium that contained 10 mM Hepes, 2 mM L-glutamine, 100 U/mL penicillin G, 100 U/mL streptomycin sulfate, 50 nM hydrocortisone, 5 pM 3,3,5-triiodo-L-thyronine, 1nM sodium selenate, 5mg/L transferrin, and 20% (wt/vol) FBS. In order to maintain AQP2 expression, the cells were grown on 24-mm transwells with 0.4 μm pores (3450, Corning). When at 70∼ 80% confluence, the cells were switched to hyperosmotic medium without FBS for 12 h before the experiments began. IMCDs were cultured in hyperosmotic medium all the time.

Luciferase Assay. Luciferase assay was performed as previously described (2). Briefly, primary IMCD cells at 60∼70% confluence were transiently transfected with an AQP2-luc reporter described

above by using LipofectAMINE 2000 (Invitrogen) according to the standard protocols by the manufacturer. β-galactosidase reporter gene, which is used as a control for transfection efficiency, was cotransfected. 24 h posttransfection, cells were treated with FXR agonist (GW4064, 2.5 μM) for 6 h or FXR adenovirus for 36 h. Then the cells were washed twice with cold PBS and lysed with 1× luciferase lysis buffer (luciferase assay kit, Promega). Luciferase activity was determined using a luminometer (Turner BioSystems). Luciferase levels in individual samples were normalized to β-galactosidase activity. All experiments were repeated at least 3 times with different cell preparations.

1. Zhang Z, et al. (2002) Proliferation and osmotic tolerance of renal inner medullary epithelial cells in vivo and in cell culture. *Am J Physiol Renal Physiol* 283(2):F302–308.

2. Zhou Y, et al. (2013) FAM3A is a target gene of peroxisome proliferator-activated receptor gamma. *Biochim Biophys Acta* 1830(8):4160–4170.

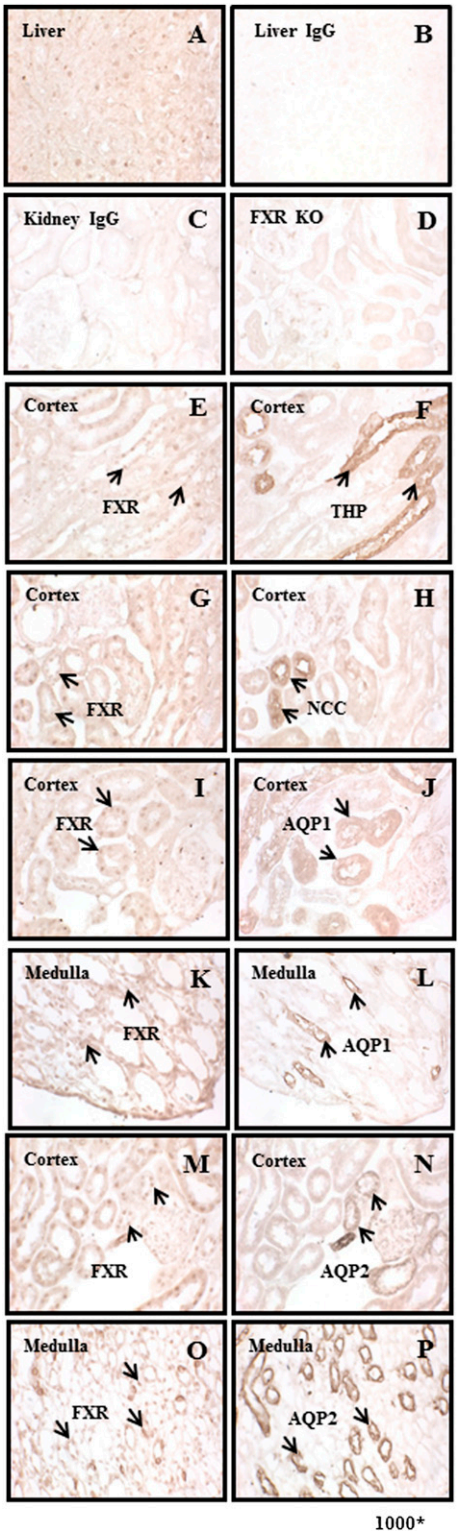

Fig. S1. Ubiquitous expression of FXR in the epithelial cells along renal tubules of nephron and collecting ducts in mouse kidney. Intrarenal distribution of FXR protein was determined by immunohistochemistry without counterstaining with H&E staining. (*A* and *B*) Normal C57BL/6 mouse liver sections were stained with (*A*) or without (*B*) the primary antibody against FXR. Note that the FXR antibody staining showed positive immunoreactivity mainly in the nuclei of liver cells (*A*); however, nonspecific IgG resulted in no specific staining (*B*). (*C*) Nonspecific IgG failed to show specific staining in the kidney. (*D*) No specific immunoreactivity was observed in FXR gene knockout mouse kidney using the FXR-specific antibody. (*E* and *F*) Colocalization of FXR (*E*) and THP in the thick ascending limbs. (*G* and *H*) FXR was expressed in the distal convoluted tubules (*G*), where NCC was expressed (*H*). (*I*–*L*) FXR was colocalized with aquaporin 1 (AQP1) in the proximal convoluted tubules of renal cortex (*I* and *J*) and the thin descending limbs of renal medulla (*K* and *L*). (*M*–*P*) FXR and AQP2 were colocalized in cortical (*M* and *N*) and medullary (*O* and *P*) collecting ducts. FXR was also expressed in interstitial fibroblasts. Arrows indicate positive staining.

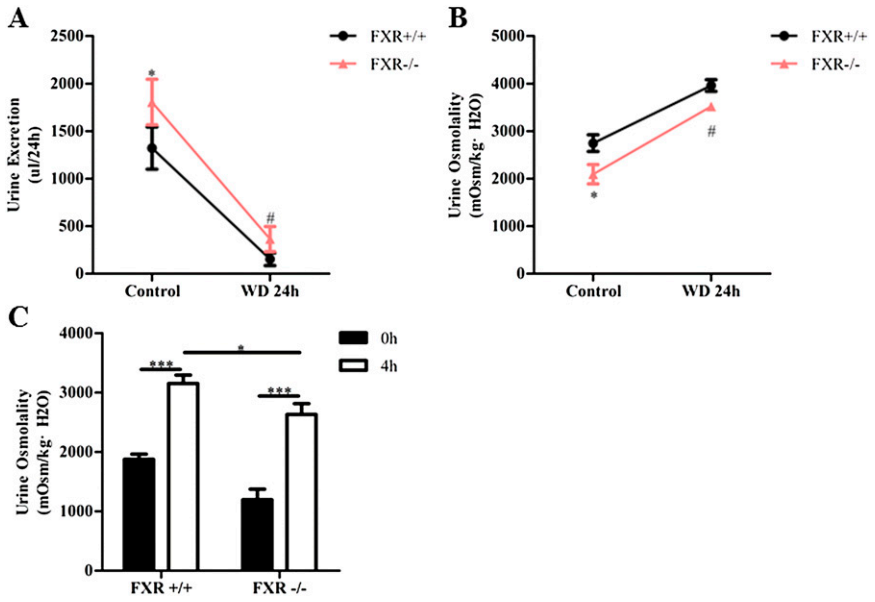

Fig. S2. Water-deprivation test in $FXR^{+/+}$ and $FXR^{-/-}$ mice. (*A* and *B*) The 24-h urine volume was significantly decreased in both $FXR^{+/+}$ mice ($n = 5$) and $FXR^{-/-}$ mice ($n = 5$) after 24-h water deprivation (WD) (*A*), with a parallel increase in urine osmolality (*B*). $^{*}P < 0.05$ vs. $FXR^{+/+}$ mice, $^{\#}P < 0.05$ vs. $FXR^{+/+}$ WD24h mice. (*C*). $FXR^{+/+}$ and $FXR^{-/-}$ mice were injected i.p. with desmopressin. Spot urine was collected by bladder massage. Urine osmolality was increased after 4 h in both groups. $^{*}P < 0.05$, $^{***}P < 0.001$ vs. 0 h. Data are presented as mean ± SEM.

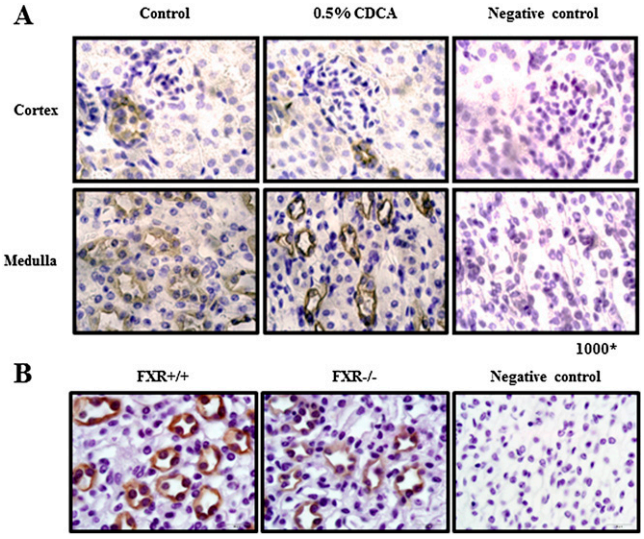

Fig. S3. Distribution of AQP2 in FXR agonist-treated $FXR^{+/+}$ and $FXR^{-/-}$ mouse kidney. (*A*) Immunohistochemical analysis of AQP2 in the kidneys of control and CDCA-treated mice. Negative controls are sections incubated with the same quantity of nonimmune rabbit IgG instead of the primary AQP2 antibody. Note that CDCA treatment had little effect on cortical AQP2 expression but significantly induced AQP2 expression and apical membrane targeting in medullary collecting duct cells. (*B*) Representative photomicrographs showing reduced AQP2 expression and apical membrane localization in medullary collecting duct cells in $FXR^{-/-}$ mice compared with $FXR^{+/+}$ mice.

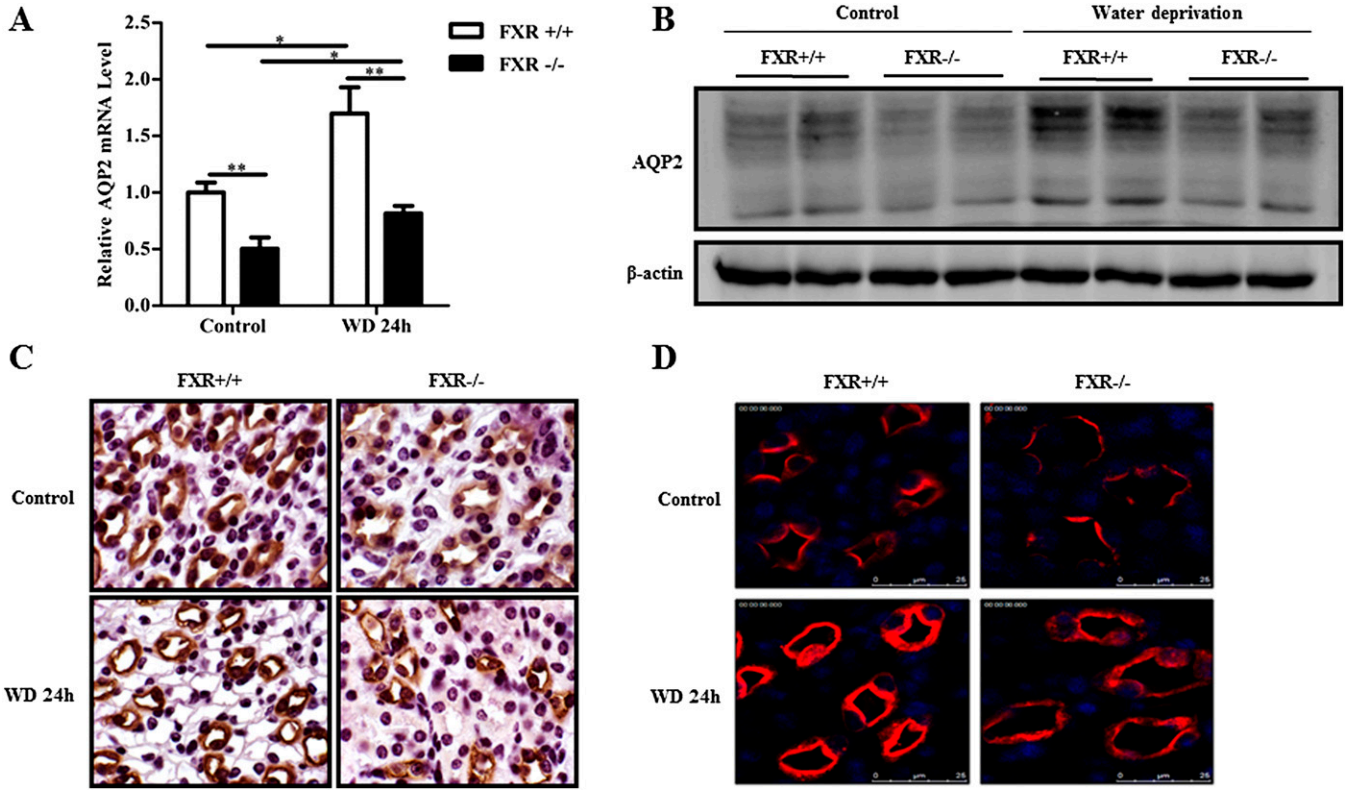

Fig. S4. Effect of water deprivation on renal AQP2 expression in $FXR^{+/+}$ and $FXR^{-/-}$ mice. (*A* and *B*). AQP2 expressions at both mRNA (*A*) and protein (*B*) levels were increased in the kidney of dehydrated $FXR^{+/+}$ mice ($n = 5$), but WD only slightly increased *AQP2* mRNA in $FXR^{-/-}$ mice ($n = 5$). $^{*}P < 0.05$, $^{**}P < 0.01$. (*C* and *D*). Immunohistochemistry (*C*) and immunofluorescence (*D*) studies of AQP2 expression in the kidney of dehydrated $FXR^{+/+}$ and $FXR^{-/-}$ mice.

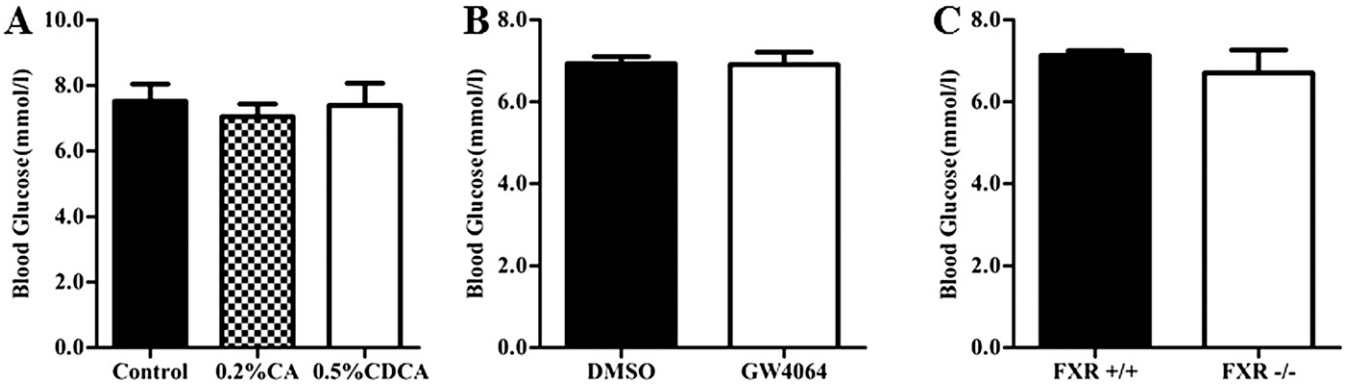

Fig. S5. Effect of FXR activation or inactivation on fasting blood glucose levels. (*A*) Fasting glucose levels of control, 0.2% CA-, and 0.5% CDCA-fed mice; $n = 5$ in each group. (*B*) GW4064 treatment ($n = 5$) had little effect on fasting blood glucose levels compared with DMSO-treated mice ($n = 6$). (*C*) No difference in fasting blood glucose levels was found between $FXR^{-/-}$ mice ($n = 7$) and $FXR^{+/+}$ mice ($n = 6$). Data are presented as mean ± SEM.

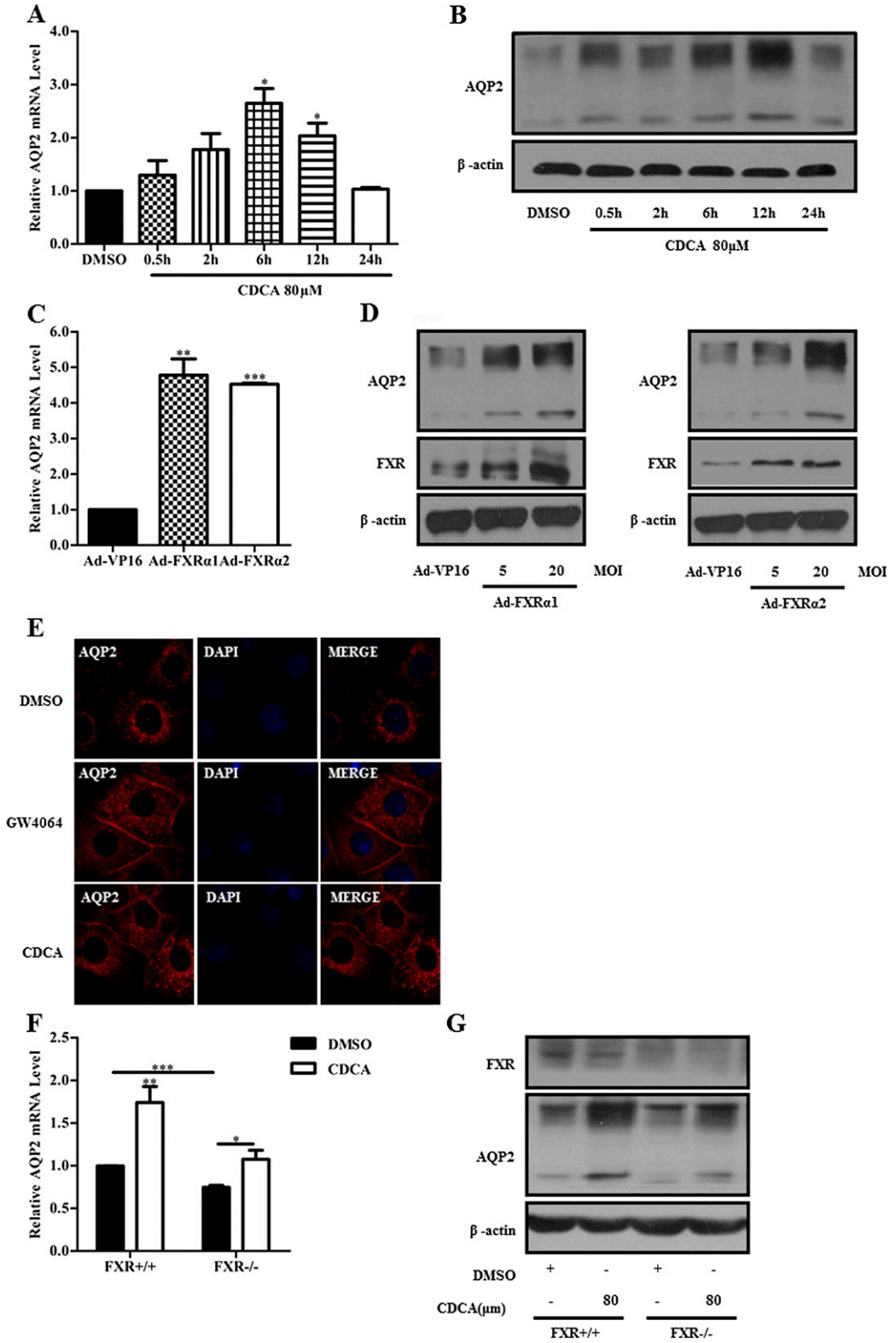

Fig. S6. Effect of FXR activation on AQP2 expression in primary IMCD cells. Primary mouse IMCD cells were treated with 80 μM CDCA for the indicated time points. (*A* and *B*) Both AQP2 mRNA (*A*) and protein (*B*) levels were markedly increased. $*P < 0.05$ vs. DMSO; $n = 3$. (*C* and *D*) Adenovirus-mediated overexpression of FXRα increased AQP2 expression at mRNA (*C*) and protein (*D*) levels. $*P < 0.05$ vs. Ad-VP16; $n = 3$. IMCD cells were infected with Ad-VP16, Ad-FXRα1, or Ad-FXRα2 for 36 h. (*E*) Immunofluorescence images of the IMCD cells treated with DMSO (*Top*), GW4064 (*Middle*), or CDCA (*Bottom*), showing increased AQP2 expression, especially membrane translocation in the cells treated with GW4064 and CDCA. (*F* and *G*) FXR gene deficiency ($FXR^{-/-}$) significantly diminished CDCA-induced AQP2 expression at the mRNA (*F*) and protein (*G*) levels in the IMCD cells. Note that CDCA treatment slightly increased AQP2 expression in $FXR^{-/-}$ IMCD cells. $*P < 0.05$ vs. DMSO treatment in $FXR^{-/-}$ IMCD cells; $**P < 0.01$ vs. DMSO treatment in $FXR^{+/+}$ IMCD cells; $***P < 0.001$ vs. DMSO treatment in $FXR^{-/-}$ IMCD cells; $n = 4$. Data are presented as mean ± SEM.

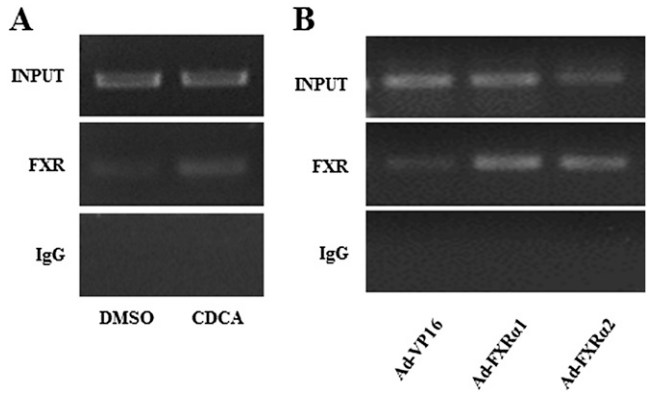

Fig. S7. CDCA activation and adenovirus-mediated overexpression of FXR increased its binding to the FXR response element site located in mouse *AQP2* gene promoter. (*A*) ChIP assay revealed that CDCA treatment for 6 h enhanced the FXR binding to the *AQP2* promoter. (*B*) Adenovirus-mediated FXR overexpression markedly increased the binding of FXR to the *AQP2* promoter. Input, positive control; FXR, anti-FXR antibody precipitated DNA; IgG, IgG precipitated DNA as negative control.

Table S1. Gene changes in the kidneys of CDCA-fed mice

Gene symbol	FC
Cyp24a1	4.91
Rarres2	3.83
1200016E24Rik	3.40
1190002H23Rik	3.18
Sgk3	3.11
8430408G22Rik	3.00
Il15ra	2.82
6030422H21Rik	2.46
AI844685	2.37
Ehf	2.37
Slc8a1	2.33
Crocc	2.14
Rpl22	2.10
Aqp2	2.09
Clca1	2.09
Mcoln3	2.06
Jarid2	2.02
Itgav	1.99
Gopc	1.98
Dnajb4	1.98
1700020I14Rik	1.98
Ergic2	1.96
Usmg5	1.95
Rgs2	1.95
E030049A20	1.95
Mnda	1.95
Clk4	1.91
Ndufb8	1.90
Arih1	1.90
Phtf2	1.89
BC089597	1.87
Fkbp5	1.87
Ppp1r8	1.84
Creb1	1.83
Usp53	1.83
Zcd2	1.83
Spink8	1.83
Nupr1	1.83
Slmo2	1.82
Slbp	1.82
Eif4e3	1.81

Table S1. Cont.

Gene symbol	FC
Trnt1	1.81
Edg2	1.80
Ipmk	1.80
Cp	1.79
Zfp36	1.79
Cebpb	1.78
Dpy19l1	1.77
EG668462	1.77
LOC675709	1.76
2610101N10Rik	1.76
LOC433762	1.76
Trim33	1.75
Vps37a	1.75
Obfc2a	1.75
Snx13	1.75
Scg5	1.75
Mitd1	1.74
Als2cl	1.73
Ppp1r16b	1.73
Cebpb	1.73
Rnmt	1.72
Rpl36a	1.72
Aqp4	1.72
Ghdc	1.71
Il15	1.70
D1Ertd622e	1.69
Cask	1.67
Tagap	1.67
Pdik1l	1.67
Gmnn	1.67
9830124H08Rik	1.67
Otud4	1.66
Cdo1	1.66
Car8	1.66
4833413G10Rik	1.66
Numb	1.65
Trp53inp1	1.65
Camta1	1.65
Ptpn13	1.65
Ttll4	1.65
Xbp1	1.64
Eif3s10	1.64
2610204L23Rik	1.64
6820431F20Rik	1.63
Foxk2	1.63
Yap1	1.63
Senp5	1.63
Gpam	1.63
1810011O10Rik	1.63
Rnf190	1.63
Ccnl2	1.63
Nqo1	1.62
Ubqln4	1.62
Ppp3cc	1.62
D16Bwg1543e	1.62
Rhebl1	1.62
Ppm2c	1.61
Ogt	1.61
Spred1	1.61
Afg3l2	1.60
Mycbp	1.60
Nt5c2	1.60

Table S1. Cont.

Gene symbol	FC
Ildr1	1.60
Klhl24	1.60
Epc2	1.60
Orc4l	1.59
Tbc1d12	1.59
Timm8b	1.59
Rbpms	1.59
6820408C15Rik	1.59
0610040D20Rik	1.58
Chka	1.58
Pdha1	1.58
Slc25a46	1.58
Gulp1	1.58
Ublcp1	1.58
l7Rn6	1.58
D10Ertd438e	1.58
Rala	1.57
2310038H17Rik	1.57
5830415L20Rik	1.57
Inoc1	1.56
S100a10	1.56
Rbm27	1.55
Prpf38b	1.55
Ifi44	1.55
Rps17	1.54
Zc3h12c	1.54
Gmfb	1.54
Senp2	1.54
C230082I21Rik	1.54
Serinc3	1.53
1810063B05Rik	1.53
Tmed2	1.53
Ube2n	1.53
Acp1	1.53
Nktr	1.53
Fundc1	1.53
Rpl22	1.53
Vps24	1.53
Dlg1	1.52
Ccdc58	1.52
Sav1	1.52
L2hgdh	1.52
Dnttip2	1.52
Ogn	1.52
Crk	1.52
Arcn1	1.52
Sgpl1	1.52
Mpp5	1.52
Eny2	1.52
Pank3	1.51
AI118064	1.51
Abca1	1.51
Akr1c12	1.51
Ranbp6	1.51
Appl1	1.50
2610209M04Rik	1.50
2610029I01Rik	1.50
2310009A05Rik	1.50
Kcnc1	0.13
BC025546	0.14
Gpsm1	0.14
4933429H19Rik	0.14
Tgm5	0.17

Table S1. Cont.

Gene symbol	FC
4833420D23Rik	0.18
Fgd3	0.20
Syvn1	0.20
Tcam1	0.20
Lce1h	0.23
Ndor1	0.24
Svep1	0.25
Spi15	0.25
LOC552878	0.25
Pex16	0.26
Gas2	0.32
Pparbp	0.35
Adamts12	0.37
Nuak2	0.39
BC003965	0.41
1810058I24Rik	0.42
Bcor	0.43
Dusp23	0.44
Src	0.45
Centg2	0.48
Srf	0.48
Cndp2	0.49
0610011L14Rik	0.51
Ddah1	0.53
Id3	0.53
Rab11fip4	0.55
Fbxo17	0.55
1700029I01Rik	0.55
Dnmt1	0.56
Hsd17b2	0.56
4930447I22Rik	0.56
Ttyh2	0.56
Elovl2	0.57
Srrm2	0.58
5730559C18Rik	0.59
Esrrg	0.59
Epn1	0.60
Aldh2	0.60
Acot2	0.60
Vps8	0.62
Dusp22	0.62
Scpep1	0.63
BC003324	0.63
D630045J12Rik	0.64
Ddr1	0.65
Pltp	0.65
Slc27a1	0.65
Fmo1	0.65
Slc25a45	0.65
Cyp51	0.65
Ubl7	0.66
Abcd1	0.66
Tlcd1	0.66
Smarcc1	0.66
Qprt	0.67
Rbed1	0.67
Ssh1	0.67
Slc7a1	0.67
Rtn4	0.67
Cd99l2	0.67
Tcp11	0.67

FC, fold change.